Proceedings of the Sixteenth International Conference on
Computational Structures Technology
Edited by: P. Iványi, J. Kruis and B.H.V. Topping
Civil-Comp Conferences, Volume 14, Paper 15.1
Civil-Comp Press, Edinburgh, United Kingdom, 2026
ISSN: 2753-3239, doi: 10.4203/ccc.14.15.1

A Variationally Consistent Force-Based Finite Element Formulation for the Dynamic Analysis of Cracked Beams Under Moving Loads

H. A. F. A. Santos

Instituto Superior de Engenharia de Lisboa, Polytechnic University of Lisbon, Portugal

Abstract

Moving loads can induce dynamic amplifications in beam-like structures that significantly exceed quasi-static predictions, especially in the presence of localized damage. This work extends a recently proposed force-based finite element formulation for beams under moving loads to cracked configurations using a physically consistent flexibility-based crack model. Cracks are represented by Dirac-delta contributions in the bending flexibility, enabling the treatment of concentrated damage without violating positive-definiteness of stiffness. The formulation, derived from a one-field variational principle dual to Hamilton's principle, yields strongly equilibrated and C0-continuous bending moment and shear force fields, which are well suited for design-oriented post-processing. Numerical results for simply-supported Euler-Bernoulli beams in both the frequency and time domains demonstrate the influence of crack location and severity on eigenfrequencies and dynamic response, and confirm the accuracy, robustness, and computational efficiency of the proposed approach.

Keywords: finite element method, force-based formulation, structural dynamics, moving loads, cracked beams, flexibility-based crack modelling

1 Introduction

Moving loads are ubiquitous in engineering structures, arising in bridges under vehicular traffic, railway tracks subjected to high-speed trains, cranes in industrial facilities, and various aerospace components. Unlike static or quasi-static actions, moving loads may induce significant dynamic amplifications, particularly in lightly damped systems and when excitation frequencies approach the natural frequencies of the structure. These effects can lead to response levels that substantially exceed static predictions and, in extreme cases, may govern serviceability and fatigue design.

Real-world structures rarely remain pristine throughout their service life. Fatigue, corrosion, and accidental damage commonly lead to the development of localized defects such as cracks, which modify stiffness distributions, alter eigenfrequencies, and redistribute internal forces. The interaction between moving loads and structural damage is therefore of central importance in safety assessment, structural health monitoring, and remaining-life estimation. Accurate numerical tools capable of capturing both dynamic amplification effects and localized stiffness degradation are essential for reliable analysis and design.

Finite element methods (FEM) are widely recognized as the standard computational framework for the analysis of beam and frame structures. Displacement-based formulations (DBF) are the most commonly adopted in practice due to their conceptual simplicity and general applicability. However, DBFs may produce bending-moment and shear-force fields that are not C^0-continuous across element boundaries [1]. While this limitation is often acceptable for global displacement predictions, it becomes problematic in damage-sensitive applications, particularly in the vicinity of cracks and under localized excitations such as moving loads, where accurate recovery of internal forces is critical for design and assessment.

Equilibrium-based or force-based finite element formulations (EBF) provide a compelling alternative, as they enforce equilibrium in a strong sense and yield internally equilibrated stress resultants [1–4]. These properties make EBF particularly attractive for problems in which internal force distributions play a central role, such as damage detection, fatigue assessment, and reliability analysis. Despite these advantages, most existing EBF developments have been confined to static analyses of beam-like structures. Only recently has a force-based finite element formulation been proposed for the dynamic analysis of undamaged beams subjected to moving loads [5], demonstrating improved internal force recovery and favourable convergence properties.

The modelling of cracks in beam structures has been extensively studied, with several approaches proposed in the literature [6]. One widely adopted method is the discrete spring model, where cracks are represented as internal rotational springs, with stiffness related to the crack size and cross-sectional geometry [7,8]. This approach allows efficient analysis of the global structural response while often disregarding local degradation effects. Another class of methods introduces singularities in the flexural stiffness using generalized Dirac delta functions, which provide a convenient mathematical framework to handle the rotation discontinuity at cracked sections [9–12].

Within this context, two main formulations have been developed: the rigidity-based approach, where singularities are imposed on the stiffness, and the flexibility-based approach, where the crack is modelled as a localized increase in compliance [13, 14]. The latter maintains the positive-definite character of the structural operator and offers a physically consistent basis for coupling crack effects with force-based finite element formulations.

In this work, the force-based finite element formulation previously developed for beam dynamics under moving loads [5] is further extended to incorporate localized damage in the form of open cracks, modelled through a physically consistent flexibility-based approach. This framework allows for the accurate computation of strongly equilibrated internal force fields in both the frequency and time domains, capturing the effects of cracks on dynamic amplification, eigenfrequencies, and transient response. To assess the performance of the proposed methodology, numerical examples on simply-supported beams are presented, demonstrating its robustness, accuracy, and computational efficiency. The results highlight the capability of the approach to serve as a reliable and physically consistent alternative to classical displacement-based formulations in damage-sensitive dynamic analyses.

2 Initial Boundary-Value Problem

The structural model considered in this work is a homogeneous, linear-elastic beam with uniform cross-section and one or more open cracks. Classical Euler-Bernoulli kinematic assumptions are adopted, namely that plane cross-sections remain plane and perpendicular to the deformed beam axis, and that shear deformation effects are neglected. The beam is assumed to be initially at rest before the application of the moving load. As a representative model problem, a simply-supported beam of length L as shown in Figure 1 is considered.

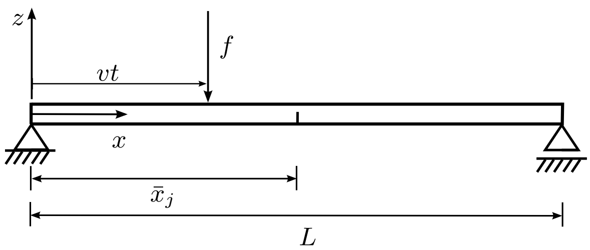

Figure 1: Simply-supported beam under moving point load.

The external excitation is a moving point load travelling along the beam at constant velocity v, which is represented in the distributional sense by a Dirac delta function,

$$f(x,t) = g(t)\,\delta(x - vt), \tag{1}$$

where $g(t)$ denotes the load amplitude. The presence of cracks is modelled through localized reductions of flexural stiffness at prescribed positions $\bar{x}_j$, as detailed below.

Under the above assumptions, the dynamic behaviour of the Euler-Bernoulli beam with moving load and localized damage is governed by the following system of partial differential equations

$$\chi - w'' = 0, \tag{2}$$

$$M'' + \dot{p} - f = 0, \qquad M' - Q = 0, \tag{3}$$

$$\frac{M}{EI(x)} - \chi = 0, \tag{4}$$

which correspond to the kinematic relation between curvature and deflection, the local equilibrium of moments and shear forces in the presence of inertial and external load contributions, and the constitutive law relating bending moment to curvature through the flexural rigidity $EI(x)$, respectively.

The governing equations are supplemented by simply-supported boundary conditions,

$$w(0,t) = 0, \qquad w(L,t) = 0, \qquad M(0,t) = 0, \qquad M(L,t) = 0, \tag{5}$$

where the first two conditions prescribe the transverse displacement at the supports (kinematic boundary conditions), while the latter two enforce vanishing bending moments at the beam ends (equilibrium boundary conditions). The problem is completed by the initial conditions

$$w(x,0) = 0, \qquad \dot{w}(x,0) = 0, \tag{6}$$

which correspond to an initially undeformed beam at rest.

Here, $w(x,t)$ denotes the transverse displacement (deflection), $\chi(x,t)$ the curvature, $M(x,t)$ the bending moment, $Q(x,t)$ the shear force, and $p(x,t)$ the translational impulse per unit length (linear momentum field). Primes ($'$) and dots ($\dot{}$) denote differentiation with respect to coordinate x and time t, respectively.

It is worth noting that the translational impulse per unit length $p(x,t)$ is directly related to the time derivative of the transverse displacement through the classical momentum-velocity relation,

$$p(x,t) = m\,\dot{w}(x,t), \tag{7}$$

where $m = \rho A$ denotes the mass per unit length of the beam, with ρ the material mass density and A the cross-sectional area. This relation provides the link between the force-based formulation, in which p appears explicitly in the equilibrium equations, and the kinematic description of the problem in terms of the displacement field $w(x,t)$. It also ensures that inertial effects induced by the moving load are consistently accounted for in the variational and finite element formulations developed in the subsequent sections.

Open cracks are modelled through a flexibility-based discrete spring representation, which introduces a localized modification of the flexural rigidity in the form [11]

$$\frac{1}{EI(x)} = \frac{1}{EI_0}\left(1 + \sum_{j=1}^{n_c} \beta_j\,\delta(x - \bar{x}_j)\right), \tag{8}$$

where EI_0 denotes the bending stiffness of the undamaged beam, n_c is the number of cracks, $\bar{x}_j$ is the location of the j-th crack, and β_j is a dimensionless parameter quantifying its severity. The crack severity coefficient is defined as

$$\beta_j = \frac{EI_0}{K_j}, \tag{9}$$

with K_j representing the equivalent rotational spring stiffness associated with the j-th crack, given by

$$K_j = 0.9\,\frac{EI_0}{d_j}\,\frac{\left(\dfrac{d_j}{h} - 1\right)^2}{\left(2 - \dfrac{d_j}{h}\right)}, \tag{10}$$

where d_j denotes the crack depth and h is the beam height. This flexibility-based representation preserves the positive-definite character of the constitutive operator and provides a physically consistent description of localized stiffness degradation.

Within the present formulation, the resulting kinematic discontinuities induced by the cracks are naturally incorporated into the generalized governing equations defined over a single, continuous computational domain for an arbitrary number of damaged sections. This unified description avoids the need for domain partitioning or the explicit enforcement of continuity conditions at crack locations, which constitutes a significant computational advantage over classical piecewise modelling strategies.

3 Variational Formulation

The force-based finite element formulation developed in this work is derived from a one-field variational principle expressed in terms of the bending-moment impulse $r(x,t)$ [5]. This choice allows equilibrium to be enforced in a strong sense at the discrete level, yielding improved accuracy in the computation of internal force fields, particularly in the presence of localized stiffness degradations induced by cracking.

In accordance with the governing equations introduced in Section 2, the linear momentum field $p(x,t)$ is related to the bending-moment impulse through

$$r''(x,t) = -\,p(x,t), \tag{11}$$

while a particular solution $M_p(x,t)$ of the bending-moment field associated with the external load $f(x,t)$ satisfies

$$M_p''(x,t) = f(x,t). \tag{12}$$

Accordingly, integrating (12) twice with respect to x yields

$$M_p(x,t) = g(t)\,(x - vt)\,H(x - vt) + C_1(t)\,x + C_2(t), \tag{13}$$

where $H(\cdot)$ denotes the Heaviside step function and $C_1(t)$, $C_2(t)$ are time-dependent integration constants. For a simply-supported beam of span L, enforcing the boundary conditions

$$M_p(0,t) = 0, \qquad M_p(L,t) = 0,$$

leads to the explicit expression

$$M_p(x,t) = g(t) \begin{cases} \dfrac{x}{L}\big(L - vt\big), & 0 \le x \le vt, \\ \dfrac{vt}{L}\big(L - x\big), & vt \le x \le L. \end{cases} \tag{14}$$

This particular solution represents the bending-moment field induced by the moving load alone and enters the force-based formulation through its time derivative $\dot{M}_p(x,t)$ appearing in the equivalent nodal load vector (28) defined below. This construction ensures that the external excitation is introduced in an equilibrated form, consistently with the underlying variational framework.

The total bending moment can therefore be decomposed as

$$M(x,t) = \dot{r}(x,t) + M_p(x,t), \tag{15}$$

so that equilibrium with respect to external loading and inertial effects is satisfied in a strong sense by construction.

The following one-field Lagrangian functional is introduced

$$\mathcal{L}_c(r,\dot{r}) = \frac{1}{2}\int_0^L \frac{r''^2}{m}\,dx - \frac{1}{2}\int_0^L \frac{\left(\dot{r} + M_p\right)^2}{EI(x)}\,dx, \tag{16}$$

where $EI(x)$ is the bending stiffness distribution incorporating the effect of cracks through the flexibility-based model introduced in Section 2. The first term represents the kinetic contribution, whereas its second term corresponds to the complementary bending energy.

By explicitly introducing the flexibility-based crack model, the functional (16) can be rewritten as

$$\mathcal{L}_c(r,\dot{r}) = \frac{1}{2}\int_0^L \frac{r''^2}{m}\,dx - \frac{1}{2}\int_0^L \frac{\left(\dot{r} + M_p\right)^2}{EI_0}\,dx - \frac{1}{2}\sum_{j=1}^{n_c} \frac{\dot{r}_j^2}{K_j}, \tag{17}$$

where $\dot{r}_j = \dot{r}(\bar{x}_j)$ denotes the time derivative of the bending-moment impulse evaluated at the location $\bar{x}_j$ of the j-th crack. The last term in (17) represents the contribution of the cracks to the complementary energy of the beam and introduces localized compliance in a physically consistent manner.

As demonstrated in [5], among all bending-moment impulses $r(x,t)$ that satisfy the equilibrium constraints, the physically admissible solution renders the functional stationary, *i.e.*,

$$\delta\mathcal{L}_c = 0, \tag{18}$$

for all admissible variations δr compatible with the prescribed boundary and initial conditions. This variational principle is dual to the classical Hamilton principle formulated in terms of the displacement field $w(x,t)$ and its time derivative. In contrast to displacement-based formulations, the present approach treats the bending-moment impulse $r(x,t)$ as the primary field, thereby enabling equilibrium to be enforced in a strong form at the discrete level.

This variational framework provides the theoretical foundation for the force-based spatial discretization presented in the following section.

4 Force-Based Finite Element Formulation

The spatial discretization of the governing equations derived from the variational principle in Section 3 is carried out using a force-based finite element formulation in which the bending-moment impulse $r(x,t)$ is taken as the primary unknown. This choice ensures that equilibrium is enforced in a strong sense at the discrete level.

4.1 Interpolation of the Bending-Moment Impulse

Consistently with the C^1-regularity requirements of the functional (17), the bending-moment impulse field is approximated within each finite element e by means of a cubic Hermite interpolation as follows

$$r_h^e(x,t) = \mathbf{N}_r(x)\,\mathbf{r}^e(t), \tag{19}$$

where $\mathbf{N}_r(x)$ denotes the vector of Hermite shape functions. The vector of element degrees-of-freedom is defined as

$$\mathbf{r}^e(t) = \begin{bmatrix} r_1^e(t) & r_1^{e\prime}(t) & r_2^e(t) & r_2^{e\prime}(t) \end{bmatrix}^T, \tag{20}$$

collecting the nodal values of the bending-moment impulse and its spatial derivative. In the force-based setting, these nodal quantities are dual to the classical kinematic degrees-of-freedom and correspond, respectively, to nodal bending moments and shear forces in the sense of impulses.

The discrete counterparts of the continuous relations introduced in Section 2,

$$p(x,t) = -\,r''(x,t), \qquad M(x,t) = \dot{r}(x,t) + M_p(x,t), \qquad Q(x,t) = M'(x,t),$$

are obtained by direct differentiation of the interpolation (19). This yields, at the element level,

$$p_h^e(x,t) = -\,\mathbf{N}_r''(x)\,\mathbf{r}^e(t), \tag{21}$$

$$M_h^e(x,t) = \mathbf{N}_r(x)\,\dot{\mathbf{r}}^e(t) + M_p(x,t), \tag{22}$$

$$Q_h^e(x,t) = \mathbf{N}_r'(x)\,\dot{\mathbf{r}}^e(t). \tag{23}$$

With this construction, the kinematic relation between curvature and bending moment, as well as the equilibrium relations between bending moment, shear force, inertia, and external loading, are satisfied pointwise within each element. This property constitutes a distinctive feature of the proposed force-based formulation and underpins the strong enforcement of equilibrium at the discrete level. As a result, equilibrated internal force fields are obtained without requiring post-processing or recovery procedures, even in the presence of localized stiffness degradations introduced by cracks.

4.2 Element Matrices

Substituting the discrete approximation (19) into the crack-consistent variational functional (16) and enforcing stationarity with respect to the nodal degrees of freedom $\mathbf{r}^e(t)$ yields the element-level equations of motion

$$\mathbf{F}^e\,\ddot{\mathbf{r}}^e(t) + \mathbf{M}^e\,\mathbf{r}^e(t) = \mathbf{d}^e(t), \tag{24}$$

where $\mathbf{F}^e$ and $\mathbf{M}^e$ denote, respectively, the element flexibility and mobility matrices associated with the bending-moment impulse field. These matrices are given by

$$\mathbf{F}^e = \int_{x_e}^{x_{e+1}} \frac{\mathbf{N}_r^T(x)\,\mathbf{N}_r(x)}{EI(x)}\,dx, \tag{25}$$

$$\mathbf{M}^e = \int_{x_e}^{x_{e+1}} \frac{\mathbf{N}_r''^T(x)\,\mathbf{N}_r''(x)}{m}\,dx, \tag{26}$$

where $EI(x)$ denotes the spatially varying bending stiffness and m is the mass per unit length.

Introducing the flexibility-based crack representation, the element flexibility matrix admits the additive decomposition

$$\mathbf{F}^e = \int_{x_e}^{x_{e+1}} \frac{\mathbf{N}_r^T(x)\,\mathbf{N}_r(x)}{EI_0}\,dx + \sum_{j=1}^{n_{ce}} \frac{\mathbf{N}_r^T(\bar{x}_j)\,\mathbf{N}_r(\bar{x}_j)}{K_j}, \tag{27}$$

where n_{ce} is the number of cracks within element e, $\bar{x}_j$ denotes the location of the j-th crack, and K_j is the associated rotational spring stiffness. This expression makes explicit the superposition of the undamaged contribution and the localized compliance induced by cracks.

The equivalent nodal load vector associated with the moving external excitation reads

$$\mathbf{d}^e(t) = -\int_{x_e}^{x_{e+1}} \frac{\mathbf{N}_r^T(x)\,\dot{M}_p(x,t)}{EI(x)}\,dx. \tag{28}$$

Consistently with the adopted crack model, this term can be decomposed into regular and localized contributions as

$$\mathbf{d}^e(t) = -\int_{x_e}^{x_{e+1}} \frac{\mathbf{N}_r^T(x)\,\dot{M}_p(x,t)}{EI_0}\,dx - \sum_{j=1}^{n_{ce}} \frac{\mathbf{N}_r^T(\bar{x}_j)\,\dot{M}_p(\bar{x}_j,t)}{K_j}, \tag{29}$$

highlighting that cracks not only affect the element flexibility operator but also introduce localized contributions to the equivalent nodal loading in a force-based formulation.

4.3 Global System of Equations

Standard finite element assembly of the element contributions (26)–(28) yields the global semi-discrete system

$$\mathbf{F}\,\ddot{\mathbf{r}}(t) + \mathbf{M}\,\mathbf{r}(t) = \mathbf{d}(t), \tag{30}$$

where $\mathbf{r}(t)$ collects all nodal bending-moment impulse degrees of freedom. Essential boundary conditions on bending moments and shear forces are imposed directly on $\mathbf{r}(t)$ and its derivatives, consistently with the continuous boundary conditions $M(0,t) = M(L,t) = 0$ and $Q(0,t) = Q(L,t) = 0$ for simply-supported beams.

4.4 Frequency-Domain Analysis

The free-vibration characteristics of the discretized system are obtained by solving the generalized eigenvalue problem

$$\big(\omega^2\mathbf{F} - \mathbf{M}\big)\,\mathbf{r} = \mathbf{0}, \tag{31}$$

which admits a countable set of eigenpairs $\{\omega_i, \mathbf{r}_i\}_{i=1}^{\infty}$, where ω_i denote the natural frequencies predicted by the proposed force-based finite element formulation and $\mathbf{r}_i$ are the associated eigenvectors. Each eigenvector represents the modal distribution of the bending-moment impulse field. The corresponding bending-moment vibration modes, as well as the kinematic mode shapes (deflection and rotation fields), are consistently recovered from $\mathbf{r}_i$ through the discrete constitutive and kinematic relations of the formulation.

4.5 Time-Domain Analysis

For transient dynamic analyses in the time domain, the global semi-discrete system (30) is integrated using the Newmark average-acceleration method with parameters $\beta = 1/4$ and $\gamma = 1/2$. This choice yields an unconditionally stable, second-order accurate time-integration scheme that preserves the equilibrium structure of the semi-discrete system [5]. At each time step, the time-dependent bending-moment impulse field $\mathbf{r}(t)$ is computed, from which all kinematic and internal force quantities — including curvature, deflection, bending moment, and shear force — are recovered directly, without the need for stress-recovery or averaging procedures.

5 Numerical Results

5.1 Simply-Supported Cracked Beam under a Moving Load

The proposed formulation is assessed through the analysis of a simply-supported beam, as illustrated in Figure 1, with a single open crack at midspan. This configuration is selected as a benchmark problem since reference solutions for cracked beams under moving loads are available in the literature.

The beam has length $L = 20$ m and rectangular cross-section with height $h = 0.20$ m and width $b = 0.20$ m. The material properties are $E = 206$ GPa and $\rho = 7800$ kg/m^3. An open crack of depth $d = 0.15$ m is introduced at the midspan location $\bar{x} = L/2 = 10$ m, corresponding to a crack severity parameter $\beta = 10/3$. The beam is subjected to a moving point load of magnitude $g = 9810$ N traveling at constant speed $v = 5$ m/s. Time integration is carried out using the Newmark average-acceleration scheme with time step $\Delta t = 4/700$ s. Uniform meshes with $n_e = 2, 4, 8, 16$, and 32 elements are considered to assess convergence.

5.1.1 Frequency-Domain Results

The convergence of the lowest four natural frequencies of the cracked beam is reported in Table 1, together with reference values taken from [15]. Even for coarse meshes, the proposed formulation provides accurate estimates of the fundamental frequency, with rapid convergence observed as the mesh is refined. For $n_e = 8$, the first four eigenfrequencies are already within less than 1% of the reference solution, and further refinement leads to negligible changes.

n_e	ω_1	ω_2	ω_3	ω_4
2	6.3511	32.5024	74.3874	148.9450
4	6.3380	29.3992	59.3992	130.0099
8	6.3372	29.2912	58.7594	117.5970
16	6.3371	29.2841	58.7121	117.1651
32	6.3372	29.2837	58.7091	117.1365
Ref. [15]	6.34	29.28	58.71	117.135

Table 1: Frequency-domain analysis: convergence of the first four eigenfrequencies.

These results confirm the ability of the force-based formulation to correctly capture the global stiffness reduction induced by the crack, as well as its influence on the modal properties of the structure. The fast convergence observed for higher modes further indicates that the discretization of the bending-moment impulse field provides an efficient representation of the underlying dynamics.

5.1.2 Time-Domain Response

The transient response induced by the moving load is examined in terms of midspan bending moment and deflection histories over the time interval $t \in [0, 4]$ s. Figure 2 shows the midspan bending moments of the damaged and undamaged beams obtained using the 2- and 8-element meshes. The midspan deflections of the damaged and undamaged beams obtained with the 8-element mesh are compared in Figure 3. As can be observed, the presence of the crack leads to a clear amplification of the bending moment response at midspan, as well as an increase in peak deflections. Moreover, the crack modifies the phase and frequency content of the transient response, reflecting the shift in eigenfrequencies induced by the localized flexibility.

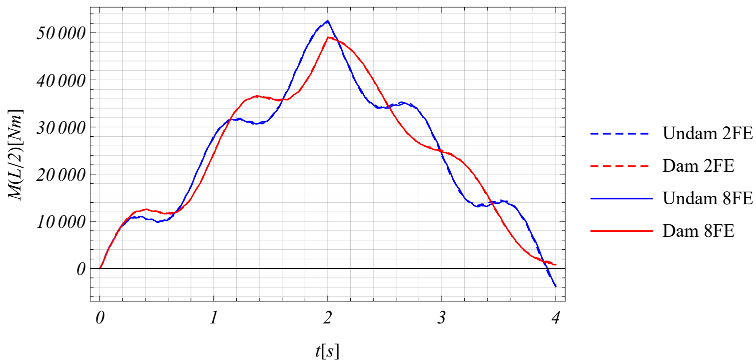

Figure 2: Time-domain analysis: mid-span bending moment solutions in the time range $t \in [0, 4]s$.

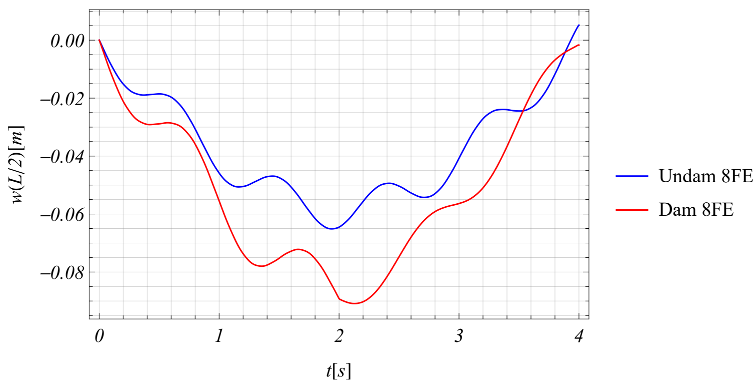

Figure 3: Time-domain analysis: mid-span deflection solutions in the time range $t \in [0, 4]s$.

5.1.3 Spatial Distributions of Internal Forces and Kinematic Fields

To further assess the quality of the computed internal force fields, spatial distributions of bending moment, shear force, deflection, and cross-section rotation along the beam are reported at $t = 2$ s for the mesh with $n_e = 8$ elements (see Figures 4, 5, 6, and 7, respectively). The bending-moment and shear-force diagrams exhibit smooth profiles along the beam span, with a localized perturbation in the vicinity of the crack location, as expected from the local reduction in flexural stiffness.

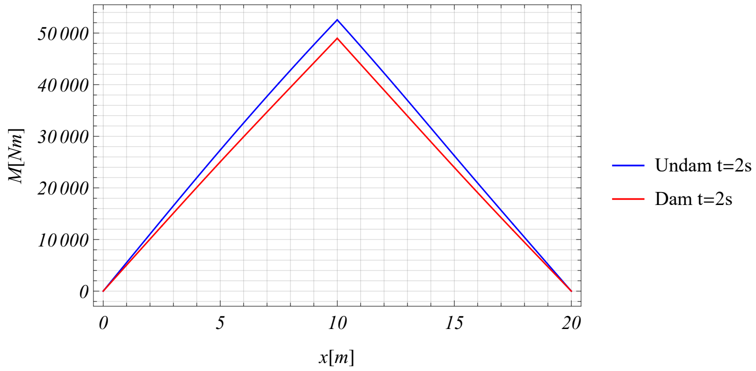

Figure 4: Time-domain analysis: bending moment distributions obtained on the 8-finite element mesh for $t = 2s$.

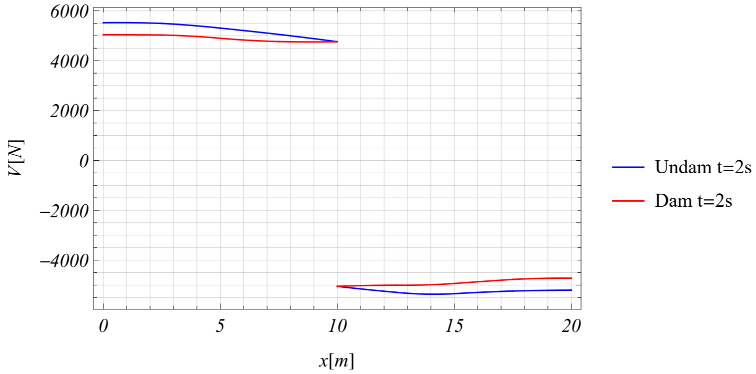

Figure 5: Time-domain analysis: shear force distributions obtained on the 8-finite element mesh for $t = 2s$.

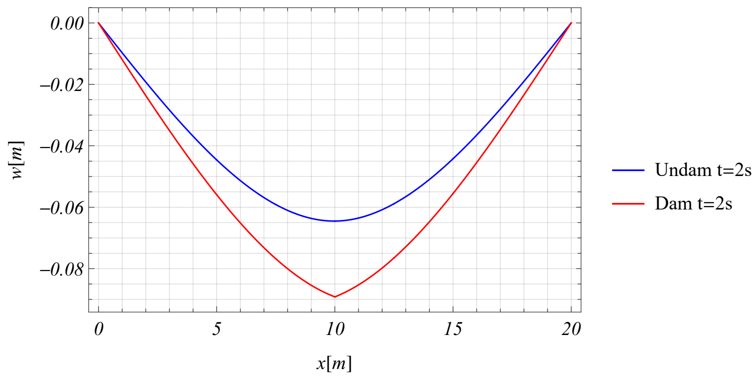

Figure 6: Time-domain analysis: deflections obtained on the 8-finite element mesh for $t = 2s$.

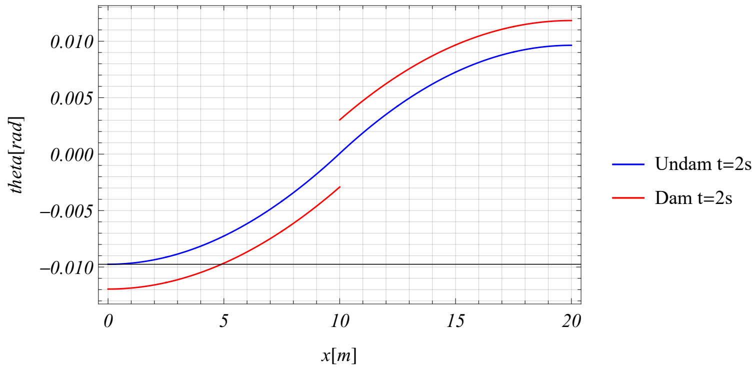

Figure 7: Time-domain analysis: cross-section rotations obtained on the 8-finite element mesh for $t = 2s$.

In contrast with classical displacement-based formulations, which may produce discontinuous or oscillatory internal force fields at element interfaces, the present force-based formulation delivers C^0-continuous bending moments and shear forces. This property is particularly advantageous for design-oriented post-processing and damage assessment, where accurate internal force distributions are essential. The deflection and rotation profiles are consistent with the internal force fields and further illustrate the localized flexibility introduced by the crack.

6 Concluding Remarks

A force-based finite element formulation for the dynamic analysis of cracked Euler–Bernoulli beams under moving loads has been presented. The method is derived from a one-field variational principle dual to Hamilton's principle and adopts the bending-moment impulse as the primary unknown, enforcing equilibrium in a strong sense at the discrete level. Localized damage is incorporated through a physically consistent flexibility-based crack model.

Numerical results for simply-supported beams with an open midspan crack show that the formulation accurately captures both global dynamics and local damage effects. Eigenfrequencies converge rapidly with mesh refinement, and time-domain analyses highlight the influence of crack location and severity on transient response. The resulting bending-moment and shear-force fields are C^0-continuous, supporting reliable post-processing and damage-sensitive assessments.

Overall, the proposed approach provides a robust and computationally efficient alternative to classical displacement-based finite element formulations for moving-load dynamics in damaged beams.

References

[1] H. A. F. A. Santos, "Variationally consistent force-based finite element method for the geometrically non-linear analysis of Euler-Bernoulli framed structures", Finite Elements in Analysis and Design, 53, 24-36, 2012.

[2] H. A. F. A. Santos, "Complementary-energy methods for geometrically non-linear structural models: an overview and recent developments in the analysis of frames", Archives of Computational Methods in Engineering, 18(4), 405-440, 2011.

[3] H. A. F. A. Santos, V. V. Silberschmidt, "Hybrid equilibrium finite element formulation for composite beams with partial interaction", Composite Structures, 108, 646-656, 2014.

[4] H. A. F. A. Santos, "Buckling analysis of layered composite beams with interlayer slip: A force-based finite element formulation", Structures, 25, 542-553, 2020.

[5] H. A. F. A. Santos, "A new finite element formulation for the dynamic analysis of beams under moving loads", Computers & Structures, 298, 107347, 2024.

[6] A. D. Dimarogonas, "Vibration of cracked structures: a state of the art review", Engineering Fracture Mechanics, 55(5), 831-857, 1996.

[7] A. K. Pandey, M. Biswas, "Damage detection in structures using changes in flexibility", Journal of Sound and Vibration, 169(1), 3-17, 1994.

[8] M. I. Friswell, J. E. T. Penny, "Crack modeling for structural health monitoring", Structural Health Monitoring, 1(2), 139-148, 2002.

[9] B. Biondi, S. Caddemi, "Closed form solutions of Euler-Bernoulli beams with singularities", International Journal of Solids and Structures, 42(9-10), 3027-3044, 2005.

[10] B. Biondi, S. Caddemi, "Euler-Bernoulli beams with multiple singularities in the flexural stiffness", European Journal of Mechanics A/Solids, 26(5), 789-809, 2007.

[11] A. Palmeri, A. Cicirello, "Physically-based Dirac's delta functions in the static analysis of multi-cracked Euler-Bernoulli and Timoshenko beams", International Journal of Solids and Structures, 48, 2184-2195, 2011.

[12] S. Caddemi, A. Morassi, "Multi-cracked Euler-Bernoulli beams: Mathematical modelling and exact solutions", International Journal of Solids and Structures, 50(6), 944-956, 2013.

[13] G. Failla, A. Santini, "On Euler-Bernoulli discontinuous beam solutions via uniform-beam Green's functions", International Journal of Solids and Structures, 44(22-23), 7666-7687, 2017.

[14] I. Fiore, F. Cannizzaro, S. Caddemi, Salvatore, I. Calio, "Distributional Green's functions for the vibrations of multi-cracked Timoshenko beams", Applied Acoustics, 228, 110302, 2025.

[15] A. Cicirello, "On the response bounds of damaged Euler-Bernoulli beams with switching cracks under moving masses", International Journal of Solids and Structures, 172, 70-83, 2019.